Impact of fine particulate matter on visibility at Incheon International Airport, South Korea

Won, Wan-Sik; Oh, Rosy; Lee, Woojoo; Kim, Ki-Young; Ku, Sungkwan; Su, Pei-Chen; Yoon, Yong-Jin

2020

Impact of Fine Particulate Matter on Visibility at Incheon International Airport, South Korea

Wan-Sik Won[1#], Rosy Oh[2#], Woojoo Lee[3], Ki-Young Kim[4], Sungkwan Ku[5], Pei-Chen Su[1*], Yong-Jin Yoon[1,6*]

[1] *School of Mechanical and Aerospace Engineering, Nanyang Technological University, Singapore 639798, Singapore*
[2] *Institute of Mathematical Sciences, Ewha Womans University, Seoul 03760, Korea*
[3] *Department of Public Health Science, Graduate School of Public Health, Seoul National University, Seoul 08826, Korea*
[4] *4D Solution Co., Ltd., Seoul 08511, Korea*
[5] *Department of Aviation Industrial and System Engineering, Hanseo University, Chungcheongnam-do 32158, Korea*
[6] *Department of Mechanical Engineering, Korea Advanced Institute of Science and Technology (KAIST), Daejeon 34141, Korea*

ABSTRACT

Low visibility at an airport causes significant flight delays, thereby reducing the airport's capacity. To better understand its contributing factors, the present study examined the visibility at Incheon International Airport, South Korea, and its relationship with meteorological conditions as well as particulate matter (PM; viz., $PM_{2.5}$ and PM_{10}) concentrations for the period of 2015–2017. A censored regression model was developed to quantitatively describe the changes in visibility, and the results demonstrated that the visibility was more strongly correlated with the concentration of $PM_{2.5}$ than PM_{10}. Specifically, the decrease in visibility was primarily determined by the interaction between $PM_{2.5}$ and meteorological factors, such as fog, haze, high temperatures, low relative humidity, and weak wind speed. A severe fog event during March 2018 was applied as a test case to validate this regression model, which estimated that the PM_{10} and $PM_{2.5}$ impaired the visibility by approximately 8.0 km (3.2 km and 4.8 km due to PM_{10} and $PM_{2.5}$, respectively) at Incheon International Airport during hazy conditions. Our findings reveal that the concentration of $PM_{2.5}$ and its interaction with meteorological factors must be considered when diagnosing and predicting reduced visibility.

Keywords: Particulate matter; Visibility; Airport; Fog; Censored regression.

INTRODUCTION

Low visibility is one of meteorological factors that severely affect flight safety and air traffic management by causing frequent flight delays and cancellations (Wong *et al.*, 2006; Lee *et al.*, 2011; FAA, 2017; Chen *et al.*, 2018). The maximum capacity of the airport is also influenced by visibility, especially when the runway visual range (RVR) is below 550 m, corresponding to the instrument landing system (ILS) Category I (CAT I) minimum (Hakkeling-Mesland *et al.*, 2010; ICAO, 2013; Jones *et al.*, 2017).

The visibility is defined as the longest distance that an object is recognized with eyesight (Hinds, 2012). It is typically affected by various types of weather events, such as rain, drizzle, snow, fog, mist, smoke, dust, sand, and haze. However, recent studies have shown that visibility is not simply influenced by the amounts of hydrometeors but also by the types and amounts of fine aerosols suspended in the air (Huang *et al.*, 2009; Hyslop, 2009). The increased gaseous pollutants and particulate matters (PM) often cause low visibility by increasing light scattering and absorption (Singh and Dey, 2012; Xiao *et al.*, 2014; Yu *et al.*, 2016).

The PM is largely grouped into the two categories, as ones with an aerodynamic diameter of 10 μm and smaller (PM_{10}) and those of 2.5 μm and smaller ($PM_{2.5}$). Depending on this size and chemical composition, PM has different impacts on visibility as each chemical constituent differently contributes to the extinction coefficient and thus the visibility (Cao *et al.*, 2012; Yu *et al.*, 2016). The significant correlation between visibility and concentration of $PM_{2.5}$ is already well documented (Pui *et al.*, 2014; Mukherjee and Toohey, 2016). Among the $PM_{2.5}$ constituents, ammonium sulfate is a key factor that determines the visibility (and the extinction

---

[#] These authors contributed equally to this work.

[*] Corresponding author.
 Tel.: 82-42-350-3233; Fax: 82-42-350-3210
 E-mail address: yongjiny@kaist.ac.kr (Y.J. Yoon);
 peichensu@ntu.edu.sg (P.C. Su)

coefficient). Other species, such as $PM_{2.5}$ ammonium nitrate and organic matter, also affect the visibility, but their impacts vary in different conditions (Zhang *et al.*, 2012; Wang *et al.*, 2013; Chen *et al.*, 2016).

The recent studies have further shown that the relationship between $PM_{2.5}$ concentration and visibility is not always linear but is modulated by relative humidity (RH) which is associated with particle hygroscopic growth (Day and Malm, 2001; Liu *et al.*, 2013; Lee *et al.*, 2016). By taking in moisture under high RH conditions, the particle size of water-soluble $PM_{2.5}$ can increase, leading to an increased extinction coefficient and reduced visibility. However, the quantitative relationship between $PM_{2.5}$ concentration and visibility under various meteorological conditions has not been established.

Due to its complexity of the process involving radiation, turbulence, droplet microphysics, dynamics, aerosol chemistry, and surface conditions, visibility forecast is quite challenging for both statistical models and numerical models (Doran *et al.*, 1999; Smith *et al.*, 2002; Gultepe *et al.*, 2007; Chmielecki and Raftery, 2011; Herman and Schumacher, 2016). Regardless of the details, both models consider fog as the most adverse meteorological condition for visibility. The prediction of fog itself, however, is difficult due to its complicated formation and maintenance processes of small spatial and short time scales. The visibility forecast becomes even more difficult if $PM_{2.5}$ and PM_{10} concentrations are taken into account. As such, most numerical weather prediction models neglect aerosol loading in determining the visibility (Clark *et al.*, 2008).

Several studies have investigated the effect of PM and weather variables on visibility by empirical modeling based on regression analysis for long-term visibility trends. Tsai (2005) developed an empirical model for visibility prediction using regression analysis with data collected for 9 years in urban areas of Taiwan, presenting the importance of PM_{10} on visibility impairment. Lin *et al.* (2012) also showed that PM_{10} and meteorological conditions affect visibility by developing an empirical regression model based on 5 years of measured air quality and meteorological parameters in megacities in China. These empirical models, however, are hardly applicable to recent low-visibility prediction at Incheon International Airport (IIA) due to the exclusion of high relative humidity (> 90%) data and the absence of $PM_{2.5}$ concentration data. The present study aims to better understand the relationship between visibility and PM concentrations especially at the airport by examining and predicting visibility impairment at IIA, South Korea, relative to PM concentration.

The IIA, located on Yeongjong Island off the west coast of the city of Incheon (Fig. 1), is one of the largest and busiest airports in East Asia. Since the airport is placed in an island downstream of industrial regions of northeastern China, its visibility is likely influenced by sea fog formed over the Yellow Sea (Gao *et al.*, 2007; Zhang *et al.*, 2009) as well as PM locally emitted or regionally transported from neighboring countries (Castellanos *et al.*, 2017; Kim *et al.*, 2018). While throughout a year the most dominant wind direction is west-northwest, on foggy days of spring, autumn, and winter east wind is more dominant (Leem *et al.*, 2005). In fact, on 23–24 December 2017, PM_{10} and $PM_{2.5}$ concentrations around IIA were as high as 110–150 µg m^{-3} and 60–120 µg m^{-3}, respectively. These have likely caused poor visibilities and record-high flight delays at the airport (KMA, 2017; NIER, 2017; MOLIT, 2018).
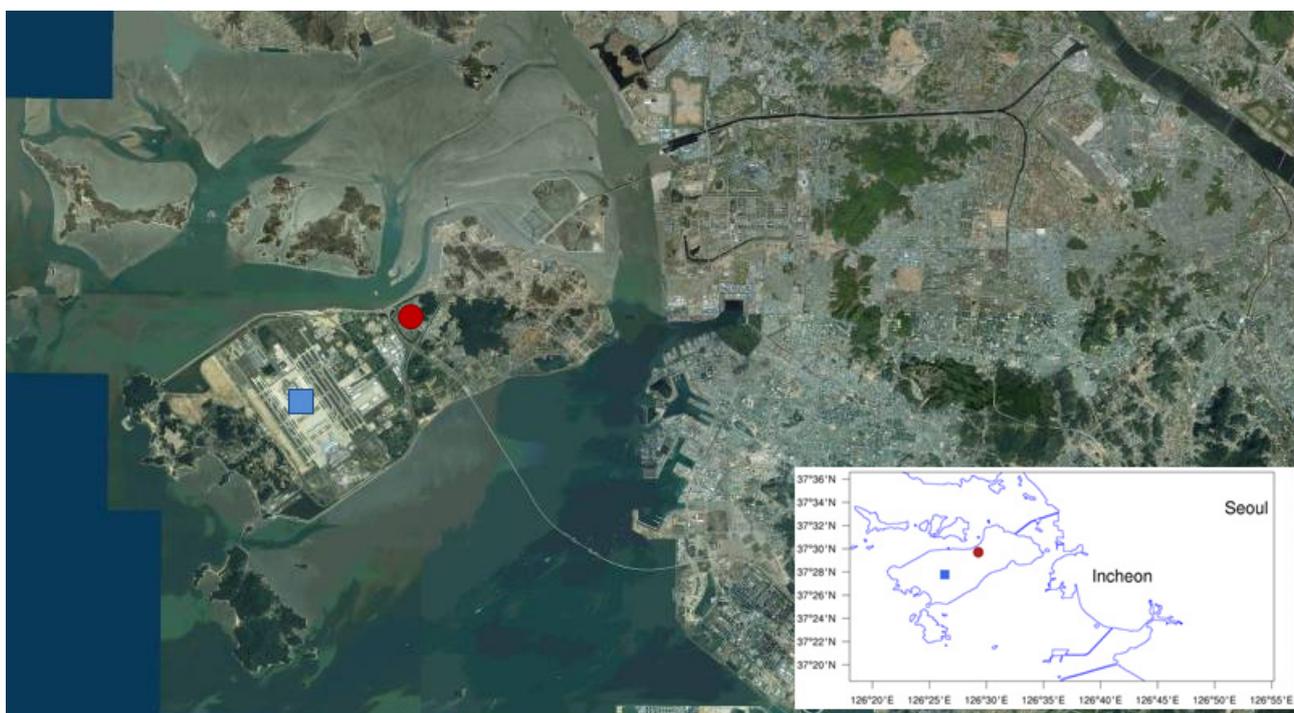
Fig. 1. The location of IIA (square mark) and the Unseo air quality monitoring station (circle mark). Map from Geospatial Information Service Platform (NGII, 2019).

By combining meteorological measurements at IIA and PM measurements at the Unseo air quality monitoring station nearby IIA (Fig. 1), we attempt to quantify the impacts of PM_{10} and $PM_{2.5}$ concentrations on airport visibility. As described in the next section, censored regression model is specifically used to evaluate the importance of PM concentration for the period of 2015–2017. Although meteorological measurements, including visibility, have been conducted since the opening of IIA in 2001, $PM_{2.5}$ measurements have been available only since 2015, as the nationwide $PM_{2.5}$ measurement network was established only in 2015 (ME, 2013; Lee, 2014).

METHODS

Data

This study investigates the relationship between weather variables from IIA and PM concentration nearby the airport (the Unseo air quality station). The locations of IIA and the Unseo station are shown in Fig. 1. The IIA (37.463°N, 126.439°E), which opened in March 2001, is placed at Yeongjong Island, 60 km west of Seoul. The collected weather data are hourly observations of visibility (VIS), present weather (WX), wind speed (WS), air temperature (TMP), and dew point temperature. The RH is estimated in regards to air temperature and dew point temperature (Lawrence, 2005). Each variable has a total of 26,304 observations for the period of 2015–2017, with no missing data intervals.

Although not shown, the 43 different types of WX observed from IIA (WMO, 2014, 2017) are classified into 8 categories in this study: haze (HZ), widespread dust (DU), mist (BR), fog (FG), drizzle (DZ), rain (RA), snow (SN), and no significant weather (NONE). It turns out that NONE is most prevalent, which accounts for 16,437 observations (62.5%). It is followed by BR (5,087; 19.3%), HZ (2,265; 8.6%), FG (463; 1.8%), DU (218; 0.8%), RA (1,546; 5.9%), SN (187; 0.7%) and DZ (101; 0.4%). This grouping is important because each weather condition has a different effect on visibility degradation and possibly leads to different interaction with PM concentration.

The Unseo air quality station (37.495°N, 126.488°E), which is located 5 km east-northeast of IIA, opened in 2007. Although both PM_{10} and $PM_{2.5}$ concentration data have been collected hourly, $PM_{2.5}$ observations began late in 2015. Over the period of 2015–2017, 10.8% of $PM_{2.5}$ observation data were unrecorded, and 7.5% for PM_{10} observations. When both $PM_{2.5}$ and PM_{10} observations are considered, missing observations are 15.4% and 22,261 observations are available. It is found that PM_{10} concentration at the Unseo station ranges from 2 to 949 μg m^{-3} with a mean value of 45.84 μg m^{-3}. Likewise, $PM_{2.5}$ concentration ranges from 1 to 111 μg m^{-3} with a mean value of 24.16 μg m^{-3}. It is important to note that the $PM_{2.5}$ mean value is larger than the annual standard of 15 μg m^{-3} from the Korean government, 12 μg m^{-3} from the U.S. government, and 10 μg m^{-3} recommended by the World Health Organization (WHO) (WHO, 2006; U.S. EPA, 2016; ME, 2018).

Censored Regression Model

To examine the effects of the PM concentrations and weather conditions on airport visibility, the censored regression model is built. A total of 6 variables, PM_{10}, $PM_{2.5}$, WS, TMP, RH, and WX, are utilized to construct the model of airport visibility. Numerous studies have revealed that WS, TMP, and RH among other weather variables have significant effects on visibility. Accordingly, Tsai (2005) and Lin *et al.* (2012) select WS, TMP, and RH as predictors excluding the data collected during rainfall. Data with RH > 90% were excluded in consideration to the particle hygroscopic effect. Yet, there is no clear reason to divide the criteria below 90% and above 90% (Malm and Day, 2001). Also, high levels of RH should not be excluded for airport low visibility as the present study focuses on not only hazy but also foggy conditions. Shen *et al.* (2015) classifies the weather conditions based on visibility and RH into three types, namely *Clear*, *Haze*, and *Fog*. Measurements with rain or snow were excluded to separate out the particle scavenging effect by precipitation. The results have shown that the degradation of visibility under foggy condition is less sensitive to the $PM_{2.5}$ concentration. As mentioned above, weather classification is essential for the examination of PM contribution to the degradation of visibility. For these reasons, WS, TMP, all level of RH, and WX were selected as the predictors in the model.

Unlike conventional regression model, censored regression model is useful for data whose range is limited. Censoring occurs when observations have incomplete information partially available. In censored regression model, the dependent variable has only the information that it is beyond the boundaries, but not how far above or below it. For example, in survival analysis, observed time from an individual still alive at the end of the study is deemed to be censored because we only know that the event time (e.g., death) is after the observed time. The dependent variable in this study, airport visibility, is reported between 0 and 10,000 m. The values larger than 9,999 m are simply set to 9,999 m (WMO, 2014) as an air operator may not care about the level of such nice weather, which means we have partial information about the visibility that it is greater than 9,999 m. Thus, it is appropriate to consider the airport visibility as censored data. As shown in Figs. 2 and 3, significant number of observations shows the visibility of 9,999 m which is upper boundary, indicating the adequate use of the censored regression model. The ranges of other variables are listed in Table 1.

The Tobit model, which is commonly used for censored data, is utilized in this study with the vglm function in R (Tobin, 1958; Yee, 2018). The vglm function which is located in VGAM (Vector Generalized Linear and Additive Models) package is for fitting vector generalized linear models including various univariate and multivariate distributions (Yee and Yee, 2019). The statistical relation between x and y is expressed as follows:

$$y_i^* = x_i'\beta + \varepsilon_i \tag{1}$$

$$y_i = \begin{cases} l & y_i^* \le l \\ y_i^* & l < y_i^* < u \\ u & y_i^* \ge u \end{cases}$$

where x_i is weather variables at IIA and PM concentrations

Table 1. Data summary of the variables, 2015–2017[a].

	VIS (m)	PM_{10} ($\mu g\ m^{-3}$)	$PM_{2.5}$ ($\mu g\ m^{-3}$)	WS (kt)[b]	TMP (°C)	RH (%)
Min.	50	2.0	1.0	0.0	–15.6	9.6
1st Qu.	7,000	27.0	13.0	4.0	3.7	49.6
Median	10,000	39.0	21.0	7.0	13.0	64.3
Mean	8,282	45.8	24.2	7.4	12.3	62.9
3rd Qu.	10,000	57.0	32.0	10.0	21.0	78.0
Max.	10,000	949.0	111.0	30.0	33.7	97.8

[a] VIS: visibility, WS: wind speed, TMP: temperature, RH: relative humidity.
[b] 1 kt = 0.5144 m s^{-1}.

at the Unseo station, y_i is airport visibility between 50 and 10,000 m, β is mean change of y_i^* when 1 unit increase in x_i, $\varepsilon_i \sim N(0, \sigma^2)$ is random error, l is 0 m, and u is 10,000 m.

When constructing regression model, multicollinearity can exist when one predictor is very close to a linear combination of other predictors. In this case, the standard errors become large and the coefficient estimates can change dramatically to the slightest changes in model configuration. As such, we first assess multicollinearity of predictors by computing cross-correlation coefficients and variance inflation factor (VIF). As summarized in Fig. 4, cross-correlation is generally small in most cases (r < 0.6). Except for WX which is a categorical variable, VIF for WS, TMP, RH, PM_{10}, and $PM_{2.5}$ is 1.3, 2.6, 1.4, 1.4, and 1.5 respectively (Table S4), which is small enough to ignore multicollinearity in this study (Montgomery *et al.*, 2012). As for WX, the box plots categorized by 8 WX levels show that each variable has little association with WX in that they are mostly similar and no significant difference is found among the categories. In the box plots of VIS, FG only has particularly low values, which is because fog is defined as being visibility of less than 1 km. That means WX might not be independent with visibility. However, as we focus not only on airport low visibility but also its variation within each category of WX it is indispensable to include WX in this study.

All models used in this study are summarized in Table 2. While Models 0–2 are not interaction models, Models 3–8 are the interaction models that include the interaction terms between weather variables and PM concentrations. Interaction indicates the influence of one factor on the effect of another factor, and vice versa. If the effects of one variable are different at different levels of another variable, there is interaction between these two variables. Previous studies have shown that impact of PM concentration on visibility is dependent on weather variables, specifically RH levels (Malm and Day, 2001; Liu *et al.*, 2013; Yu *et al.*, 2016), which implies that the PM may influence weather affecting visibility degradation in different ways. Thus, interaction term is incorporated in the model to better predict visibility impairment. Model 8 has minimum Akaike information criterion (AIC) and is reasonably considered as optimal model in this study (Akaike, 1974). AIC consists of a goodness-of-fit measure and model complexity and thus can be used even for non-nested model comparison. Furthermore, we have conducted a likelihood ratio test (LRT) to compare two nested models provided smaller model is special case of the larger model. For example, Models 0–7 are nested within Model 8, which the former

models can be represented as Model 8 with zero coefficients for a subset of independent variables. The larger model and the smaller model are called as *full model* and *reduced model*, respectively. LRT is for testing the null hypothesis, "H_0: Reduced model is adequate," versus the alternative hypothesis, "H_1: Not H_0," with the test statistic given as:

$$LRT = -2(\log L_r - \log L_f) \tag{2}$$

where L_r is a likelihood function for reduced model and L_f is a likelihood function for full model.

Table 3 summarizes the result of LRT with p-value at the 0.05 level of significance. Row and column of the table represent the reduced model and the full model, respectively. In the table, NA indicates that the two models are not nested so LRT cannot be obtained.

For example, we can compare Model 4 ($PM_{2.5}$ excluded) and Model 8 using LRT as Model 8 contains all the parameters of Model 4, $PM_{2.5}$ and $PM_{2.5}$'s interactions so that the two models are nested. Based on the LRT with p-value less than 0.0001, there is a significant evidence that the null hypothesis, "H_0: Model 4 is adequate," is rejected and Model 8 is more appropriate to explain the dataset.

In the case of comparing Model 5 (PM_{10} excluded) to Model 7 (PM_{10}'s interactions excluded), based on the LRT with p-value larger than 0.1, there is not a significant evidence that the null hypothesis, "H_0: Model 5 is adequate," is rejected. In addition, the result of comparing Model 7 to Model 8 shows that Model 8 is more appropriate to explain the dataset. These two results imply that PM_{10} does not make significant effect but PM_{10}'s interaction does. In other words, we can presume that PM_{10} affects the prediction of airport visibility through the relationships between other variables. As shown in Model 8, there are a total of 34 independent parameters. These include all the interaction terms between PM concentrations and weather parameters (WS, TMP, RH, WX).

RESULTS AND DISCUSSION

Relationship between PM and Weather Variables

The characteristic of airport visibility is shown in Fig. 2. Significant number of observations indicating the visibility of 9,999 m normally has the value more than 9,999 m. The rate of fog observations less than 1 km of visibility is relatively low. However, the density of low visibility below 500 m (0.042) is more frequent than that between 500 m and 1,000 m (0.025). This implies that there are more chances of

Table 2. Variables applied to model design and selection of optimum model.

No.	Censored regression model[a]	# of parameters	AIC[c]
0	$[VIS] = \beta_{01}[TMP] + \beta_{02}[RH] + \beta_{03}[WS] + 26.23$	5	58,348
1	$[VIS] = \beta_{11}[PM_{10}] + \beta_{12}[PM_{2.5}] + \beta_{13}[TMP] + \beta_{14}[RH] + \beta_{15}[WS] + 31.62$	7	50,408
2	$[VIS] = \beta_{21}[PM_{10}] + \beta_{22}[PM_{2.5}] + \beta_{23}[WX] + \beta_{24}[TMP] + \beta_{25}[RH] + \beta_{26}[WS]^b + 25.49$	14	32,833
3	$[VIS] = \beta_{31}[PM_{10}] + \beta_{32}[PM_{2.5}] + \beta_{33}[TMP] + \beta_{34}[RH] + \beta_{35}[WS]$ $+ \beta_{36}[PM_{10}{:}TMP] + \beta_{37}[PM_{10}{:}RH] + \beta_{38}[PM_{10}{:}WS]$ $+ \beta_{39}[PM_{2.5}{:}TMP] + \beta_{310}[PM_{2.5}{:}RH] + \beta_{311}[PM_{2.5}{:}WS] + 31.54$	13	48,469
4	$[VIS] = \beta_{41}[PM_{10}] + \beta_{42}[WX] + \beta_{43}[TMP] + \beta_{44}[RH] + \beta_{45}[WS]$ $+ \beta_{46}[PM_{10}{:}WX] + \beta_{47}[PM_{10}{:}TMP] + \beta_{48}[PM_{10}{:}RH] + \beta_{49}[PM_{10}{:}WS] + 31.54$	23	33,244
5	$[VIS] = \beta_{51}[PM_{2.5}] + \beta_{52}[WX] + \beta_{53}[TMP] + \beta_{54}[RH] + \beta_{55}[WS]$ $+ \beta_{56}[PM_{2.5}{:}WX] + \beta_{57}[PM_{2.5}{:}TMP] + \beta_{58}[PM_{2.5}{:}RH] + \beta_{59}[PM_{2.5}{:}WS] + 31.54$	23	32,286
6	$[VIS] = \beta_{61}[PM_{10}] + \beta_{62}[PM_{2.5}] + \beta_{63}[WX] + \beta_{64}[TMP] + \beta_{65}[RH] + \beta_{66}[WS]$ $+ \beta_{67}[PM_{10}{:}WX] + \beta_{68}[PM_{10}{:}TMP] + \beta_{69}[PM_{10}{:}RH] + \beta_{610}[PM_{10}{:}WS] + 31.54$	24	32,195
7	$[VIS] = \beta_{71}[PM_{10}] + \beta_{72}[PM_{2.5}] + \beta_{73}[WX] + \beta_{74}[TMP] + \beta_{75}[RH] + \beta_{76}[WS]$ $+ \beta_{77}[PM_{2.5}{:}WX] + \beta_{78}[PM_{2.5}{:}TMP] + \beta_{79}[PM_{2.5}{:}RH] + \beta_{710}[PM_{2.5}{:}WS] + 31.54$	24	32,391
8	$[VIS] = \beta_{81}[PM_{10}] + \beta_{82}[PM_{2.5}] + \beta_{83}[WX] + \beta_{84}[TMP] + \beta_{85}[RH] + \beta_{86}[WS]$ $+ \beta_{87}[PM_{10}{:}WX] + \beta_{88}[PM_{10}{:}TMP] + \beta_{89}[PM_{10}{:}RH] + \beta_{810}[PM_{10}{:}WS]$ $+ \beta_{811}[PM_{2.5}{:}WX] + \beta_{812}[PM_{2.5}{:}TMP] + \beta_{813}[PM_{2.5}{:}RH] + \beta_{814}[PM_{2.5}{:}WS] + 31.54$	34	32,072

[a] [VIS], [PM_{10}], [$PM_{2.5}$], [WS], [TMP], and [RH] stand for visibility (km), PM_{10} concentration ($\mu g\ m^{-3}$), $PM_{2.5}$ concentration ($\mu g\ m^{-3}$), wind speed (kt), temperature (°C) and relative humidity (%), respectively.
[b] [WX] has 8 levels: [NONE], [FG], [BR], [HZ], [DU], [DZ], [RA], and [SN], which have the value of 0 or 1.
[c] AIC: Akaike information criterion.

Table 3. p-Values from the likelihood ratio test for Models 0–8.

Reduced Model	Full Model								
	0	1	2	3	4	5	6	7	8
0	-	< 0.0001	< 0.0001	< 0.0001	< 0.0001	< 0.0001	< 0.0001	< 0.0001	< 0.0001
1		-	< 0.0001	< 0.0001	NA	NA	< 0.0001	< 0.0001	< 0.0001
2			-	NA	NA	NA	< 0.0001	< 0.0001	< 0.0001
3				-	NA	NA	NA	NA	< 0.0001
4					-	NA	< 0.0001	NA	< 0.0001
5						-	NA	> 0.1	< 0.0001
6							-	NA	< 0.0001
7								-	< 0.0001
8									-

visibility restrictions below ILS CAT I minimum (550 m) under foggy conditions. The relationship of PM concentrations and the visibility is shown in Fig. 3. Reporting scale for aerodrome visibility varies with visibility. It is reported in steps of 1,000 m for 5 km or more, but less than 10 km (WMO, 2014). In this study, we assume that the visibility is continuous variable. Considerable number of low-visibility observations is plotted with low level of PM concentrations, which indicates low visibility is not simply influenced by particle amount suspended in the air, but by other meteorological conditions related to high RH. The remarkable PM_{10} distribution with more than 400 $\mu g\ m^{-3}$ in Fig. 3 indicates heavy Asian Dust case in February 2015 (Park *et al.*, 2016).

Fig. 4 shows the characteristics of all the variables in the datasets, and their relationships with one another. VIS represents the airport visibility which is the response variable in the analysis. The figures shown at the diagonal position represent the histogram of each variable. Except for WX, the figures above and below the diagonal position show correlation and scatter plots between two variables. Since WX is a categorical variable, which has 8 levels of NONE, HZ, DU, BR, FG, DZ, RA, and SN, the figures above and below the WX histogram show box plots of each variable categorized by 8 WX levels. The matrix represents that none of the variables are highly correlated with each other. RH is most negatively correlated with the visibility (–0.58) and followed by $PM_{2.5}$ (–0.49) and PM_{10} (–0.26). As mentioned, $PM_{2.5}$ concentration is more correlated with visibility than PM_{10}. The correlation coefficient between $PM_{2.5}$ and PM_{10} is 0.56. To verify if it is appropriate to use PM_{10} and $PM_{2.5}$, as PM_{10} includes $PM_{2.5}$ in its definition, we have assessed multicollinearity between the variables and shown that the selection of the variables is valid for analysis. It might be because PM_{10} is more correlated with coarse particles ($PM_{10\text{-}2.5}$) than fine particles ($PM_{2.5}$).

Table 4(a) shows results of the optimal model with both PM_{10} and $PM_{2.5}$ incorporated. The estimation of $PM_{2.5}$ coefficient is highly significant with the p-value less than 0.0001 while that of PM_{10} is not significant with p-value of 0.3542. Instead, PM_{10} interaction with WX is highly significant, which indicates PM_{10} affect visibility through its
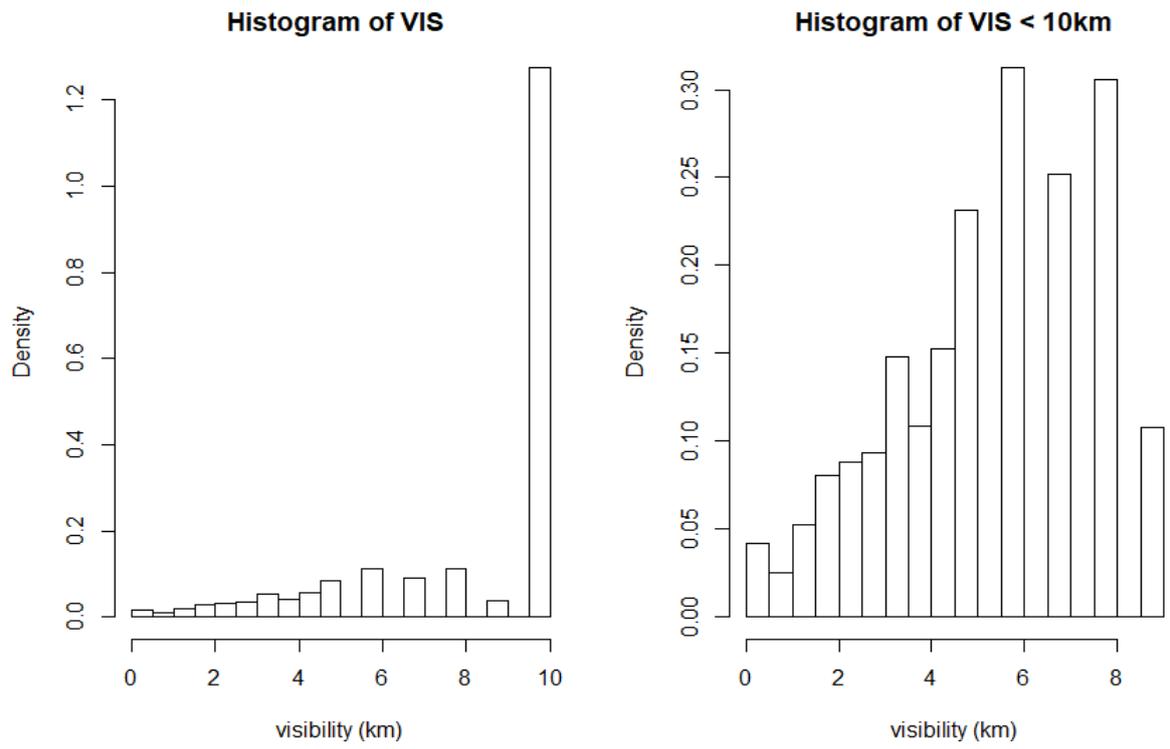
Histogram of VIS

Histogram of VIS < 10km

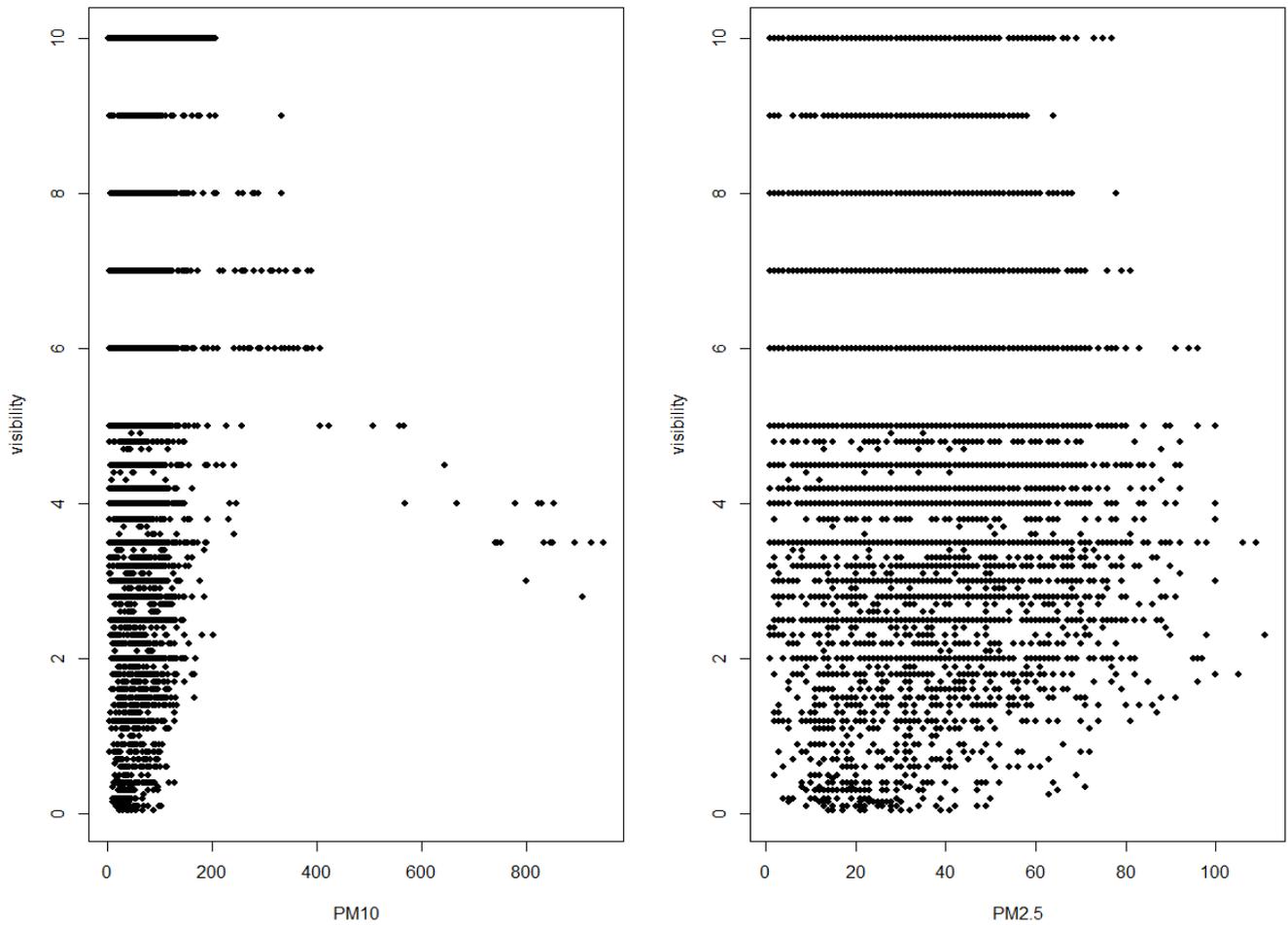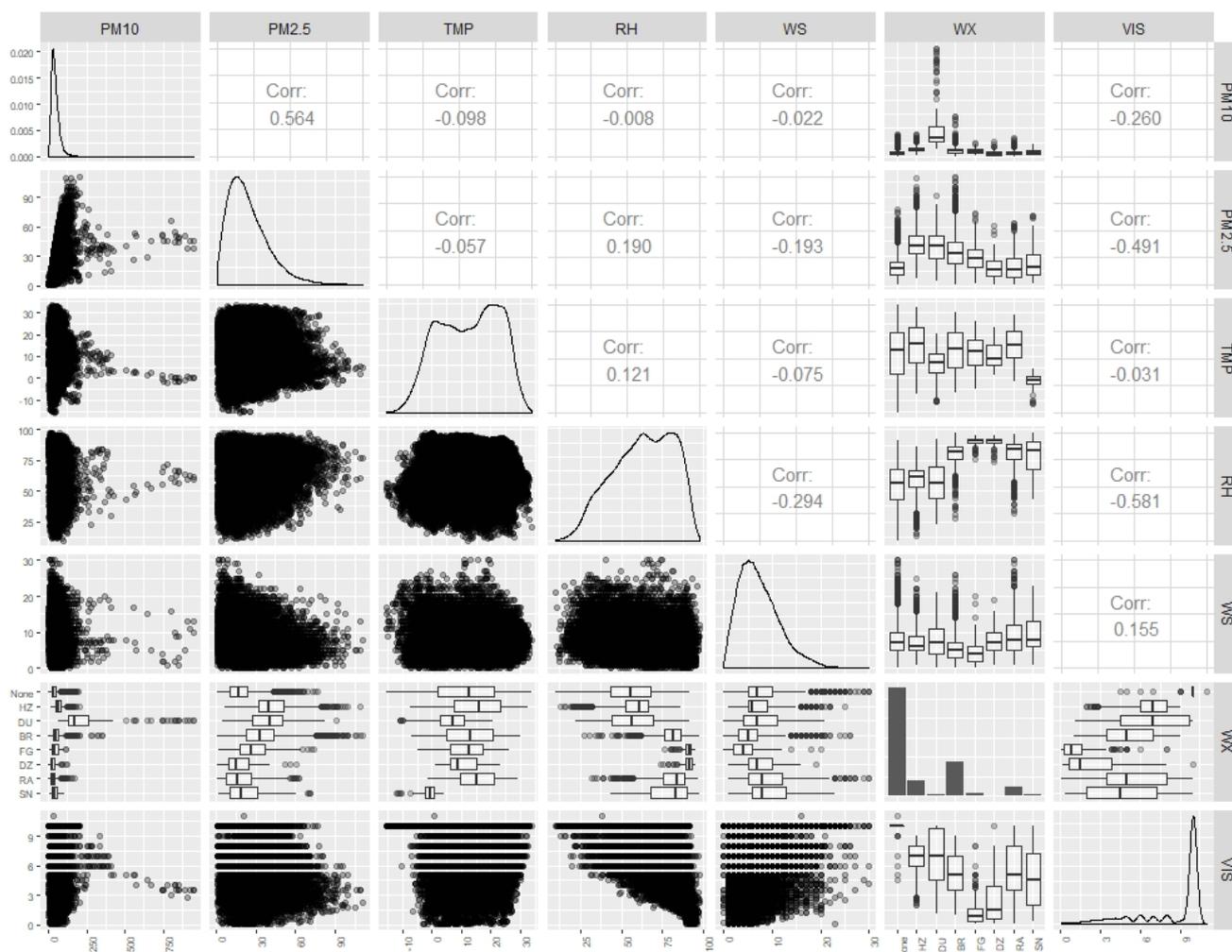Fig. 2. Distribution of observed visibility (km) at IIA, 2015–2017.

Fig. 3. Scatter plot of visibility (km) and PM concentration (μg m^{-3}) at IIA, 2015–2017.

Fig. 4. Matrix of plots and correlation coefficient among 7 variables. The upper panel above the diagonal shows correlation coefficients. The lower panel below the diagonal gives their scatter plots. The histograms of each variable are shown in the diagonal line. For WX, the upper and lower panel (the two are the same) gives box plots of each variable categorized by 8 WX levels: NONE, HZ, DU, BR, FG, DZ, RA, and SN in order. Units are as follows: PM_{10} (µg m^{-3}), $PM_{2.5}$ (µg m^{-3}), TMP (°C), RH (%), WS (kt), and VIS (km) respectively.

relationships between other weather variables. All weather variables have strong significance. As for interaction term, PM_{10} with HZ, FG, DZ, and RH is highly significant with low p-value less than 0.01. Similarly, $PM_{2.5}$ has significant interaction with HZ, FG, TMP, RH, and WS with low p-value. Among 7 WX variables in $PM_{2.5}$ interaction, HZ and FG have significant interaction with $PM_{2.5}$ concentration (p-value with 0.0005 and 0.0029 respectively). These results show that $PM_{2.5}$ needs to be taken into consideration for visibility diagnosis and prediction in both hazy and foggy conditions.

Each coefficient shows the influence of each variable on visibility. In general, all 7 weather variables have negative effect on visibility. Weather effects on visibility for each variable calculated from Table 4(a) are summarized in Table 5. They show that the specific weather effect can be interpreted along with the concentrations of $PM_{2.5}$ and PM_{10}. Temperature effect ($0.02414 + 0.00001122$ [PM_{10}] $- 0.001378$ [$PM_{2.5}$]) is dependent on $PM_{2.5}$ concentration, which indicates TMP has a positive effect on visibility under very low $PM_{2.5}$ concentration

but not under high $PM_{2.5}$ concentration due to the negative interaction between $PM_{2.5}$ and TMP (-0.001378). For example, as $PM_{2.5}$ concentration increases, the relationship between temperature and visibility tends to be diminished. When considering diurnal variation in temperature and visibility, this implies that high $PM_{2.5}$ concentration could delay visibility improvement with even increasing temperature. Relative humidity effect ($-0.2098 + 0.0004021$ [PM_{10}] $+ 0.001789$ [$PM_{2.5}$]) is mostly negative for both PM_{10} and $PM_{2.5}$ concentration levels for the period of 2015–2017, but depending on PM concentration. This means the higher PM concentration delays the improvement in visibility from decrease of relative humidity. This might be because that aerosols account for light extinction more than hydrometeors do under dry condition when temperature increases under high PM concentration. Wind speed effect ($-0.06750 + 0.00005788$ [PM_{10}] $+ 0.001878$ [$PM_{2.5}$]) also varies with $PM_{2.5}$ concentration. Under low $PM_{2.5}$ concentration, wind accounts for visibility degradation, whereas weak wind is

associated with low visibility during high $PM_{2.5}$ concentrations. According to the estimation coefficients, if both PM_{10} and $PM_{2.5}$ concentration are doubled from the mean of 45.8 µg m^{-3} and 24.2 µg m^{-3} to 91.6 µg m^{-3} and 48.4 µg m^{-3} respectively in 40% of RH, 10°C of TMP, and 10 kt of WX of hazy conditions, PM impact accounts for 2.9 km decrease in visibility. Likewise, both doubled PM_{10} and $PM_{2.5}$ from the mean in 60% of RH would reduce the visibility by 1.7 km.

Table 4. Estimation results of the proposed censored regression model (Model 8) with the comparison to that of $PM_{2.5}$ removed (Model 4).

	(a) Model 8				(b) Model 4			
	Estimate	Std. Error	p-Value[a]		Estimate	Std. Error	p-Value	
(Intercept):1	31.54	0.5727	0.0000	***	27.11	0.4757	0.0000	***
(Intercept):2	0.5093	0.007839	0.0000	***	0.5775	0.007826	0.0000	***
PM_{10}	0.02289	0.02471	0.3542		–0.04625	0.009598	0.0000	***
$PM_{2.5}$	–0.2445	0.03164	0.0000	***		N/A		
WXHZ	–9.147	0.4111	0.0000	***	–8.643	0.3651	0.0000	***
WXDU	–6.824	0.5600	0.0000	***	–8.451	0.4232	0.0000	***
WXBR	–6.804	0.3832	0.0000	***	–7.460	0.3438	0.0000	***
WXFG	–11.08	0.4321	0.0000	***	–11.58	0.3991	0.0000	***
WXDZ	–9.294	0.5280	0.0000	***	–9.969	0.4969	0.0000	***
WXRA	–6.793	0.3907	0.0000	***	–7.323	0.3523	0.0000	***
WXSN	–8.449	0.4769	0.0000	***	–8.686	0.4521	0.0000	***
TMP	0.02414	0.005219	0.0000	***	0.02004	0.004705	0.0000	***
RH	–0.2098	0.004966	0.0000	***	–0.1576	0.003788	0.0000	***
WS	–0.06750	0.009509	0.0000	***	–0.01860	0.007190	0.0097	**
PM_{10}:WXHZ	–0.06612	0.02438	0.0067	**	–0.02202	0.008879	0.0131	*
PM_{10}:WXDU	–0.05189	0.02433	0.0329	*	–0.0001866	0.008826	0.9831	
PM_{10}:WXBR	–0.05766	0.02430	0.0176	*	–0.03218	0.008745	0.0002	***
PM_{10}:WXFG	–0.06725	0.02538	0.0081	**	–0.008821	0.009573	0.3569	
PM_{10}:WXDZ	–0.07722	0.02902	0.0078	**	–0.02535	0.01241	0.0410	*
PM_{10}:WXRA	–0.05296	0.02458	0.0312	*	–0.03905	0.008998	0.0000	***
PM_{10}:WXSN	–0.03617	0.02577	0.1605		–0.02228	0.01054	0.0346	*
PM_{10}:TMP	0.00001122	0.00009899	0.9097		–0.0006563	0.00007345	0.0000	***
PM_{10}:RH	0.0004021	0.00005171	0.0000	***	0.0006180	0.00004542	0.0000	***
PM_{10}:WS	–0.00005788	0.00009585	0.5460		0.0004039	0.00008771		***
$PM_{2.5}$:WXHZ	0.1034	0.02962	0.0005	***				
$PM_{2.5}$:WXDU	0.04113	0.03060	0.1789					
$PM_{2.5}$:WXBR	0.03919	0.02934	0.1816					
$PM_{2.5}$:WXFG	0.09498	0.03184	0.0029	**		N/A		
$PM_{2.5}$:WXDZ	0.07870	0.04227	0.0627					
$PM_{2.5}$:WXRA	0.009793	0.03004	0.7444					
$PM_{2.5}$:WXSN	0.01760	0.03217	0.5843					
$PM_{2.5}$:TMP	–0.001378	0.0001869	0.0000	***		N/A		
$PM_{2.5}$:RH	0.001789	0.0001420	0.0000	***		N/A		
$PM_{2.5}$:WS	0.001878	0.0003042	0.0000	***		N/A		

[a] *, **, and ***: Significant at the 0.05, 0.01, and 0.001 probability level, respectively.

Table 5. Weather effects on visibility for each variable.

Weather	Effect on visibility (km)
HZ	$-9.147 - 0.06612$ [PM_{10}] $+ 0.1034$ [$PM_{2.5}$]
DU	$-6.824 - 0.05189$ [PM_{10}] $+ 0.04113$ [$PM_{2.5}$]
BR	$-6.804 - 0.05766$ [PM_{10}] $+ 0.03919$ [$PM_{2.5}$]
FG	$-11.08 - 0.06725$ [PM_{10}] $+ 0.09498$ [$PM_{2.5}$]
DZ	$-9.294 - 0.07722$ [PM_{10}] $+ 0.07870$ [$PM_{2.5}$]
RA	$-6.793 - 0.05296$ [PM_{10}] $+ 0.009793$ [$PM_{2.5}$]
SN	$-8.449 - 0.03617$ [PM_{10}] $+ 0.01760$ [$PM_{2.5}$]
TMP	$+ 0.02414 + 0.00001122$ [PM_{10}] $- 0.001378$ [$PM_{2.5}$]
RH	$-0.2098 + 0.0004021$ [PM_{10}] $+ 0.001789$ [$PM_{2.5}$]
WS	$-0.06750 - 0.00005788$ [PM_{10}] $+ 0.001878$ [$PM_{2.5}$]

To evaluate the difference between the effect of $PM_{2.5}$ and PM_{10} on visibility, we tried to remove $PM_{2.5}$ concentration data from the model assuming that $PM_{2.5}$ was not measured before 2015. The results are shown in Table 4(b). The largest difference from the optimal model is the coefficient for the interaction of PM_{10} with FG, which has small value with low significance. While the interaction effect of both PM_{10} and $PM_{2.5}$ with FG is highly significant (p-value of 0.0081 and 0.0029 respectively) in the optimal model as shown in Table 4(a), when $PM_{2.5}$ concentration data is not available, the interaction effect of PM_{10} with fog is not significant (with p-value of 0.3569). Such difference from the model implies that both $PM_{2.5}$ and PM_{10} should be considered to properly investigate the PM impact on visibility.

Developing an Optimal Model for Visibility

Visibility impairment is diagnosed from the estimation coefficient in the model as shown in Table 4(a). Model 8 in Table 2 shows the developed optimal censored regression model capable of visibility diagnosis considering various weather variables and interactions with PM concentration. The model has 14 coefficients in total, which practically increases to 32 because WX has been categorized into 7 types of weather conditions except for NONE as shown in Table 4(a). As interaction terms are incorporated into the model, all 32 coefficients are used to explain visibility degradation in various weather and PM conditions. Interaction terms are crucial features that explain the roles of fine and coarse PM and such complexity is worthy of being incorporated to properly evaluate the impact of meteorological conditions.

To verify the developed model using the meteorological and air quality data in 2015–2017, the visibility estimation equation was applied to low-visibility case of IIA in 2018. Data for only the term January–May 2018 are available at the present study. Fog observations were made on chosen 16 days during the 5 months. Severe dense fog with low visibility below ILS Category III landing minimum (RVR < 175 m) were observed on 4 days for two fog cases (11–12 and 26–27 March). Since this study aims to improve the airport visibility prediction, the worst foggy event of 11–12 March associated with high concentrations of PM was chosen for validating the model. On those days, haze was dominant during the day on 11 March and the visibility began to fall from the evening resulting in the lowest visibility of 100 m, which lasted for 9 hours until the early morning. After fog dissipated, hazy conditions remained with maximum visibility of 4,000 m on 12 March. As for PM_{10} and $PM_{2.5}$ concentration, the selected cases showed high levels of PM concentration. Hourly variation of PM_{10} and $PM_{2.5}$ concentrations on 11–13 March are shown in Fig. 5.

The changes in observed and modeled visibility for selected case is shown in Fig. 6. The grey solid line with circle mark and red solid line indicate observation and the optimal model's simulated visibility respectively. The black, green long-dash, and orange two-dash lines are from the non-interaction models. The blue dashed line is from the Forecast Systems Laboratory (FSL) method for reference, which is calculated by temperature (T), dew point temperature (T_d) and relative humidity (RH) as follows (Doran *et al.*, 1999):

$$VIS\,(\text{km}) = 9654 \times \frac{T - T_d}{RH^{1.75}} \qquad (3)$$

Although the error between observation and simulated visibility has quite a bit of variation by individual hours and the overall visibility tends to be underestimated, the model successfully reproduces the patterns of visibility trends associated with high PM concentrations. Specifically, the PM impact on visibility at 1 p.m. on 12 March 2018 with 39% of RH, 110 µg m⁻³ of PM_{10}, and 63 µg m⁻³ of $PM_{2.5}$ is –8.0 km (–3.2 km by PM_{10} and –4.8 km by $PM_{2.5}$) by
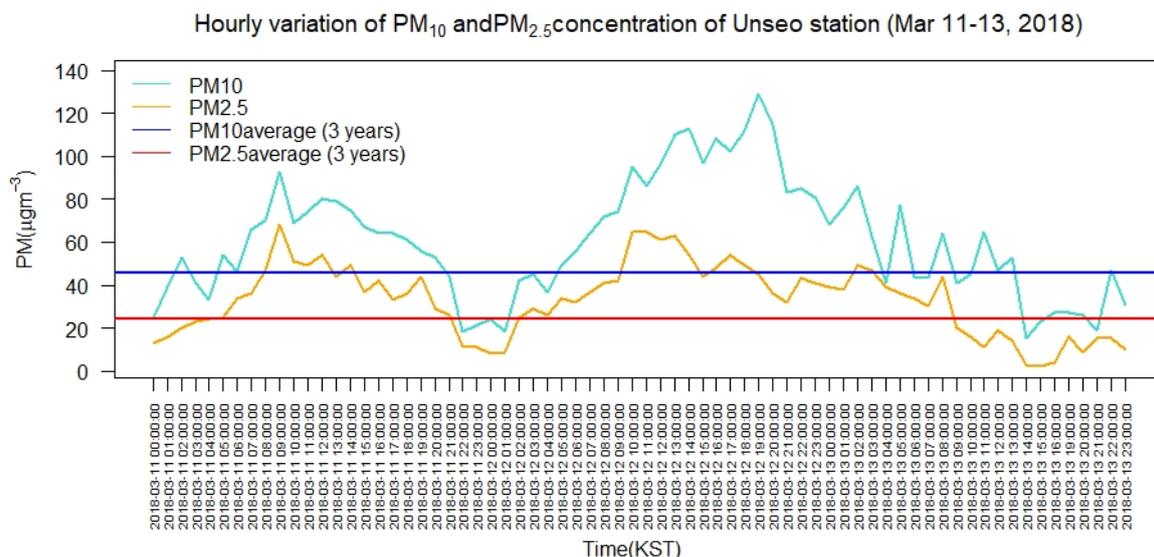
Fig. 5. Hourly variation of PM_{10} (blue) and $PM_{2.5}$ (orange) concentrations of Unseo station on 11–13 March 2018. Solid straight line indicates average PM concentration of PM_{10} and $PM_{2.5}$ for 2015–2017 respectively.
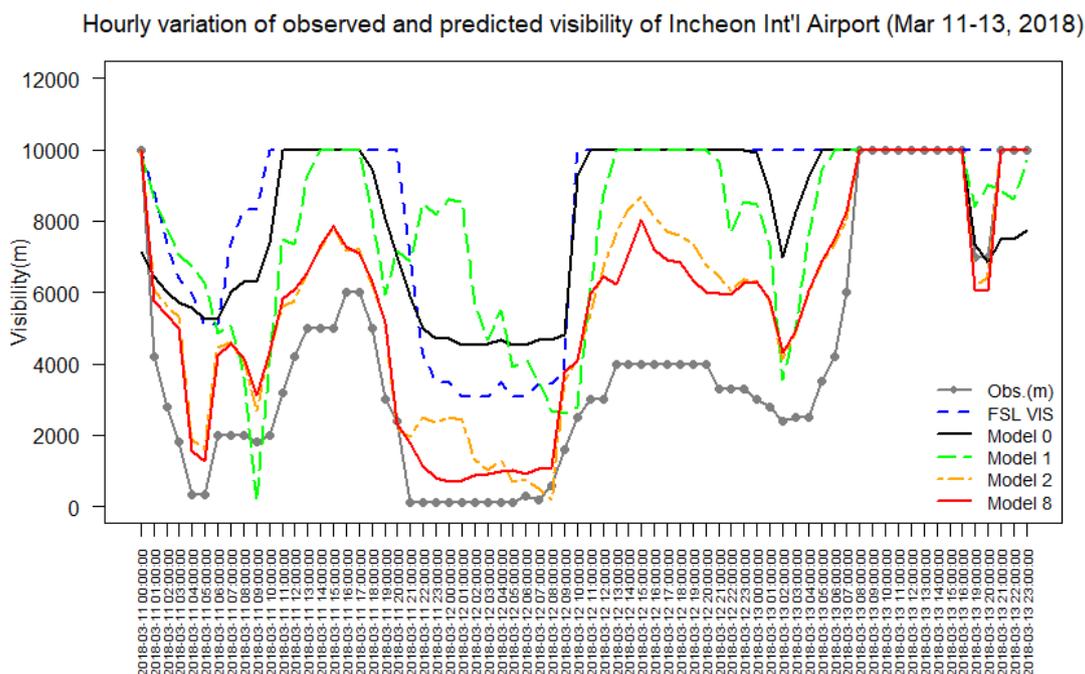
Fig. 6. Hourly variation of observed and predicted visibility of IIA on 11–13 March 2018 for FSL method, non-interaction models (Models 0, 1, and 2), and optimal interaction model (Model 8).

calculating the coefficients from the model. As shown above, the proposed model in the present study could be useful for improving visibility prediction by considering weather variables associated with PM_{10} and $PM_{2.5}$ concentrations. Accurate measurement and prediction of PM concentrations is important factor as well. Especially, fine PM such as $PM_{2.5}$ and even $PM_{1.0}$ has been found to contribute substantially to visibility degradation (Zhao *et al.*, 2013; Shen *et al.*, 2015).

Fig. 7 shows hourly variation of $PM_{2.5}$ concentration measured in Incheon city area on 11–12 March 2018. The high PM concentration at the Unseo station during the day on 11 March recedes back to annual average and even lower after 9 p.m., while other monitoring stations in Incheon area still have high level of $PM_{2.5}$ concentration. This big difference of PM measurement may relate to fog at IIA generated from 9 p.m. The proposed model shows that PM concentration is relatively low in high-RH conditions with low visibility, which indicates that some fine particles grow beyond 10 µm in fog condition by the process of particle hygroscopic growth (Malm and Day, 2001; Shen *et al.*, 2015). Fig. 8 shows observed and simulated hourly visibility from January to May 2018 in case of PM level "bad" based on the criterion issued by the Korean government (ME, 2018). The correlation coefficient of observed and simulated visibility is 0.76, which suggests that the proposed model using the data of 2015–2017 at IIA simulates the visibilities for the data collected in 2018 with significant accuracy for a single selected verification period. Meanwhile, possible errors from uncertainty such as low significance of PM_{10} coefficient on the model and inaccuracy of PM measurement in nearby site may still remain.

Although PM data collected from the Unseo station, 5 km east-northeast of IIA, is in the boundary of visibility observation from the airport, it is not the same location where other weather variables are measured. Thus, either PM data need to be collected from IIA point or spatial distribution of PM concentration should be verified for the future. Currently available PM monitoring station operated by government is sparsely distributed, which may not accurately represent the PM concentration gradient between the two points (Escobedo and Nowak, 2009; Bell *et al.*, 2010). Fig. 7 presents the differences of the measured PM concentrations at Incheon city area are considerably high between stations.

CONCLUSIONS

This study examines the quantitative relationship between visibility at an airport and meteorological conditions in light of PM concentrations. Unlike previous studies, not only the direct relationships between visibility and meteorological variables but also the latter's interactions with PM across the full range of RH are considered. Our results, which are based on three years (2015–2017) of weather and air quality observations at IIA and the Unseo air monitoring station, reveal that the visibility is determined by the concentration of $PM_{2.5}$ rather than of PM_{10}, being significantly affected, in particular, by $PM_{2.5}$'s interaction with haze, fog, high temperatures, low relative humidity, and weak wind. When the $PM_{2.5}$ concentration is high, it mitigates the effects of increasing temperature and decreasing humidity on visibility. The wind speed also displays a positive correlation with the visibility during high $PM_{2.5}$ concentrations.

To address the interplay with PM in the relationship between visibility and weather, a simple censored regression model was developed. This model, which was based on hourly observations for the period of 2015–2017, was applied to a
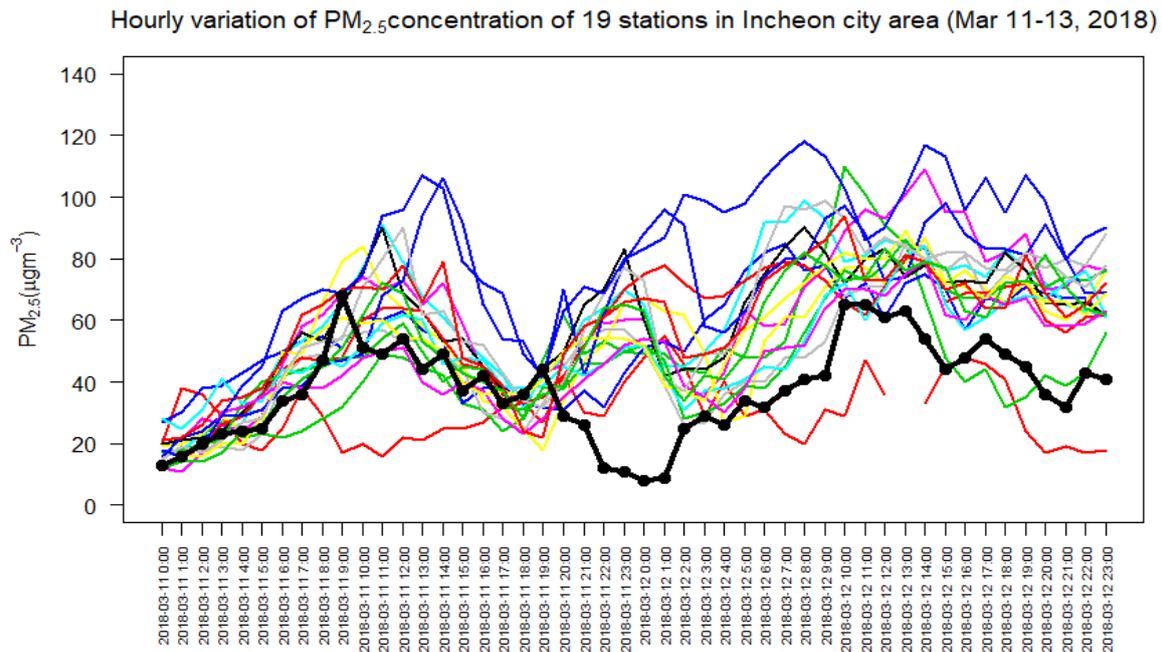
Fig. 7. Hourly variation of $PM_{2.5}$ concentrations measured at 19 air monitoring stations in Incheon city area on 11–12 March 2018. The thick solid line with circle mark indicates from Unseo station.
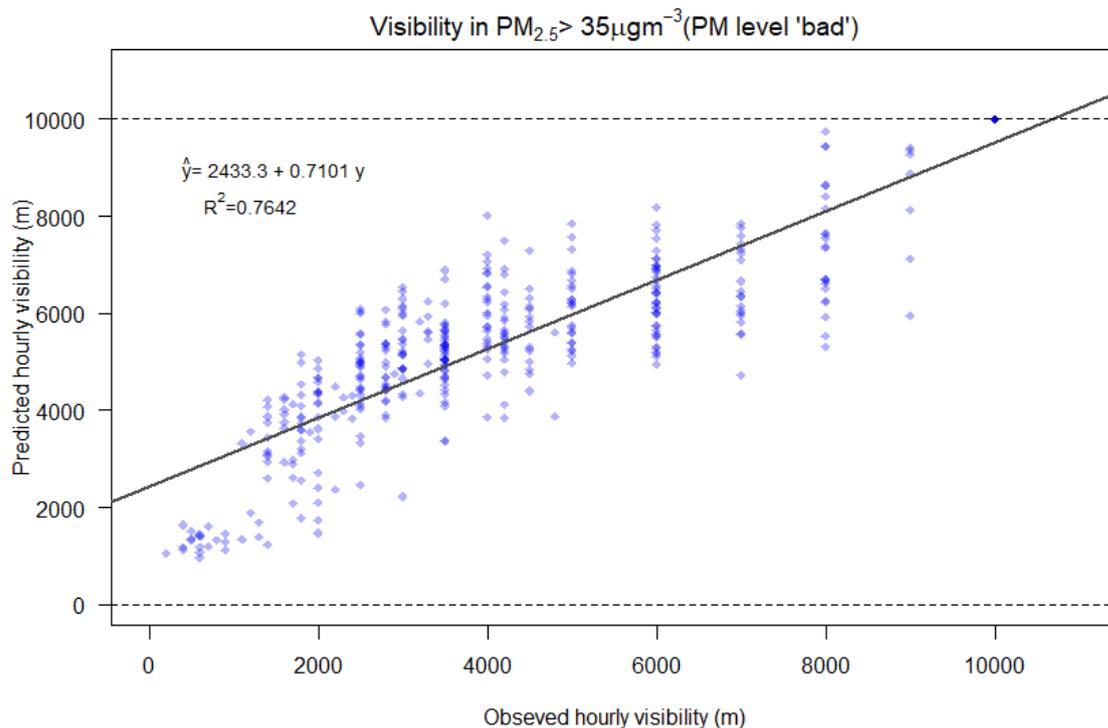
Fig. 8. Observed and predicted hourly visibility for $PM_{2.5} > 35$ µg m^{-3} at IIA using censored regression model (Model 8 of Table 2) from 1 January till 25 May 2018.

low-visibility case at IIA during 2018 and successfully reproduced the changes in visibility associated with high concentrations of PM. Predicting the quantitative impact of PM_{10} and $PM_{2.5}$ under various weather conditions, it estimated that high PM concentrations during afternoon haze on the selected day reduced the visibility by as much as 8.0 km

(3.2 km from PM_{10} and 4.8 km from $PM_{2.5}$). These results accentuate the significant role of $PM_{2.5}$ and its interaction with meteorological factors in impairing visibility, which must be considered when diagnosing and forecasting the latter.

At the moment, general weather prediction models ignore aerosol loading when predicting visibility. Likewise, air quality

prediction models, which are basically chemical transport models, do not incorporate the interactions between meteorological variables and aerosols. In the model we developed, meteorological conditions are simply prescribed from numerical weather prediction model output. Although it is not easy to implement visibility-aerosol interactions in a model, multiple outputs can be combined to improve visibility forecasting. Applying our censored regression model to outputs may enhance the accuracy of visibility prediction at an airport, an approach that will be tested in a future study.

ACKNOWLEDGMENTS

SUPPLEMENTARY MATERIAL

Supplementary data associated with this article can be found in the online version at http://www.aaqr.org.

REFERENCES

Akaike, H. (1974). A new look at the statistical model identification. *IEEE Trans. Autom. Control* 19: 716–723.

Bell, M.L., Ebisu, K. and Peng, R.D. (2010). Community-level spatial heterogeneity of chemical constituent levels of fine particulates and implications for epidemiological research. *J. Exposure Sci. Environ. Epidemiol.* 21: 372.

Cao, J.J., Wang, Q.Y., Chow, J.C., Watson, J.G., Tie, X.X., Shen, Z.X., Wang, P. and An, Z.S. (2012). Impacts of aerosol compositions on visibility impairment in Xi'an, China. *Atmos. Environ.* 59: 559–566.

Castellanos, P., Da Silva, A. and Longo-De Freitas, K. (2017). Korea-United States Air Quality (KORUS-AQ) Campaign. Global Modeling and Assimilation Office, NASA, USA.

Chen, X., Lai, S., Gao, Y., Zhang, Y., Zhao, Y., Chen, D., Zheng, J., Zhong, L., Lee, S.C. and Chen, B. (2016). Reconstructed light extinction coefficients of fine particulate matter in rural Guangzhou, Southern China. *Aerosol Air Qual. Res.* 16: 1981–1990.

Chen, Y., Yu, J., Tsai, S.B. and Zhu, J. (2018). An empirical study on the indirect impact of flight delay on China's economy. *Sustainability* 10: 357.

Chmielecki, R.M. and Raftery, A.E. (2011). Probabilistic visibility forecasting using bayesian model averaging. *Mon. Weather Rev.* 139: 1626–1636.

Clark, P.A., Harcourt, S.A., Macpherson, B., Mathison, C.T., Cusack, S. and Naylor, M. (2008). Prediction of visibility and aerosol within the operational Met Office Unified Model. I: Model formulation and variational assimilation. *Q. J. R. Meteorolog. Soc.* 134: 1801–1816.

Day, D.E. and Malm, W.C. (2001). Aerosol light scattering measurements as a function of relative humidity: A comparison between measurements made at three different sites. *Atmos. Environ.* 35: 5169–5176.

Doran, J.A., Roohr, P.J., Beberwyk, D.J., Brooks, G.R., Gayno, G.A., Williams, R.T., Lewis, J.M. and Lefevre, R.J. (1999). The MM5 at the AF Weather Agency – New products to support military operations. Proceedings of 8th Conference on Aviation, Range, and Aerospace Meteorology, Dallas, TX, 1999, pp. 115–119.

Escobedo, F.J. and Nowak, D.J. (2009). Spatial heterogeneity and air pollution removal by an urban forest. *Landscape Urban Plann.* 90: 102–110.

Federal Aviation Administration (FAA) (2017). FAQ: Weather Delay, https://www.faa.gov/nextgen/programs/weather/faq/, Last Access: 29 March 2018.

Gao, S., Lin, H., Shen, B. and Fu, G. (2007). A heavy sea fog event over the Yellow Sea in March 2005: Analysis and numerical modeling. *Adv. Atmos. Sci.* 24: 65–81.

Hakkeling-Mesland, M., Beek, B.V., Bussink, F., Mulder, M. and van Paassen, M. (2010). Evaluation of an autonomous taxi solution for airport operations during low visibility conditions. National Aerospace Laboratory NLR, The Netherlands.

Herman, G.R. and Schumacher, R.S. (2016). Using reforecasts to improve forecasting of fog and visibility for aviation. *Weather Forecasting* 31: 467–482.

Hinds, W.C. (2012). *Aerosol Technology: Properties, Behavior, and Measurement of Airborne Particles*. John Wiley & Sons, New York.

Huang, W., Tan, J., Kan, H., Zhao, N., Song, W., Song, G., Chen, G., Jiang, L., Jiang, C., Chen, R. and Chen, B. (2009). Visibility, air quality and daily mortality in Shanghai, China. *Sci. Total Environ.* 407: 3295–3300.

Hyslop, N.P. (2009). Impaired visibility: The air pollution people see. *Atmos. Environ.* 43: 182–195.

International Civil Aviation Organization (ICAO) (2013). *ICAO 9365 Manual of All-Weather Operations (Doc 9365 AN/910)*, Third edition ed. International Civil Aviation Organization, Canada.

Jones, J.C., DeLaura, R., Pawlak, M., Troxel, S. and Underhill, N. (2017). 14th USA/Europe Air Traffic Management Research and Development Seminar (ATM2017), Seattle, USA.

Kim, H., Zhang, Q. and Heo, J. (2018). Influence of intense secondary aerosol formation and long-range transport on aerosol chemistry and properties in the Seoul Metropolitan Area during spring time: Results from KORUS-AQ. *Atmos. Chem. Phys.* 18: 7149–7168.

Korea Meteorological Administration (KMA) (2018). Aerodrome Meteorological Observation Retrieve,

https://data.kma.go.kr/data/air/selectAmosList.do?pgmN o=574, Last Access: 18 Feburary 2018

Lawrence, M.G. (2005). The relationship between relative humidity and the dewpoint temperature in moist air: A simple conversion and applications. *Bull. Am. Meteorol. Soc.* 86: 225–234.

Lee, J.W., Ko, K.K., Kwon, T.S. and Lee, K.K. (2011). A study on the critical meteorological factors influencing the flight cancelation and delay: Focusing on domestic airports. *J. Korean Soc. Aviat. Aeronaut.* 19: 29–37.

Lee, M. (2014). An analysis on the concentration characteristics of $PM_{2.5}$ in Seoul, Korea from 2005 to 2012. *Asia-Pac. J. Atmos. Sci.* 50: 585–594.

Lee, S.Y., Gan, C. and Chew, B.N. (2016). Visibility deterioration and hygroscopic growth of biomass burning aerosols over a tropical coastal city: A case study over Singapore's airport. *Atmos. Sci. Lett.* 17: 624–629.

Leem, H., Lee, H. and Lee, S. (2005). The analysis of the characteristics of the fog generated at the Incheon int'l airport. *J. Korean Meteorol. Soc.* 41: 1111–1123.

Lin, M., Tao, J., Chan, C.Y., Cao, J.J., Zhang, Z.S., Zhu, L.H. and Zhang, R.J. (2012). Regression analyses between recent air quality and visibility changes in megacities at four haze regions in China. *Aerosol Air Qual. Res.* 12: 1049–1061.

Liu, X., Gu, J., Li, Y., Cheng, Y., Qu, Y., Han, T., Wang, J., Tian, H., Chen, J. and Zhang, Y. (2013). Increase of aerosol scattering by hygroscopic growth: Observation, modeling, and implications on visibility. *Atmos. Res.* 132–133: 91–101.

Malm, W.C. and Day, D.E. (2001). Estimates of aerosol species scattering characteristics as a function of relative humidity. *Atmos. Environ.* 35: 2845–2860.

Ministry of Environment (ME) (2013). Metropolitan Air Quality Control Master Plan. Ministry of Environment, Korea.

Ministry of Environment (ME) (2018). Standards for Air Pollution Prediction and Announcement. Ministry of Environment, Korea.

Ministry of Land, Infrastructure and Transport (MOLIT) (2018). Air Passenger Trend: Flight Delay and Cancellation by the Airports, In *Aviation Market*, The Ministry of Land, Infrastructure and Transport, Korea.

Montgomery, D.C., Peck, E.A. and Vining, G.G. (2012). *Introduction to Linear Regression Analysis*. John Wiley & Sons, Hoboken, New Jersey.

Mukherjee, A. and Toohey, D.W. (2016). A study of aerosol properties based on observations of particulate matter from the U.S. embassy in Beijing, China. *Earth's Future* 4: 381–395.

National Geographic Information Institute (NGII) (2019). Geospatial Information Service Platform, http://map.ngii. go.kr/ms/map/NlipMap.do, Last Access: 14 June 2019.

National Institute of Environmental Research (NIER) (2017). Statistics Information: Air Quality Data Retrieve, https://www.airkorea.or.kr/web/pastSearch, Last Access: 18 Feburary 2018.

Park, M.E., Cho, J.H., Kim, S., Lee, S.S., Kim, J.E., Lee, H.C., Cha, J.W. and Ryoo, S.B. (2016). Case study of the heavy Asian dust observed in late february 2015. *Atmosphere* 26: 257–275. (in Korean with English Abstract)

Pui, D.Y.H., Chen, S.C. and Zuo, Z. (2014). $PM_{2.5}$ in China: Measurements, sources, visibility and health effects, and mitigation. *Particuology* 13: 1–26.

Shen, X.J., Sun, J.Y., Zhang, X.Y., Zhang, Y.M., Zhang, L., Che, H.C., Ma, Q.L., Yu, X.M., Yue, Y. and Zhang, Y.W. (2015). Characterization of submicron aerosols and effect on visibility during a severe haze-fog episode in Yangtze River Delta, China. *Atmos. Environ.* 120: 307–316.

Singh, A. and Dey, S. (2012). Influence of aerosol composition on visibility in megacity Delhi. *Atmos. Environ.* 62: 367–373.

Smith, T.L., Benjamin, S.G. and Brown, J.M. (2002). Preprints, 10th Conf. on Aviation, Range, and Aerospace Meteorology, Portland, OR, American Meteorological Society, JP1, 2002, Citeseer.

Tobin, J. (1958). Estimation of relationships for limited dependent variables. *Econometrica* 26: 24–36.

Tsai, Y.I. (2005). Atmospheric visibility trends in an urban area in Taiwan 1961–2003. *Atmos. Environ.* 39: 5555–5567.

U.S. EPA (2016). NAAQS Table, https://www.epa.gov/crite ria-air-pollutants/naaqs-table, United States Environmental Protection Agency, Last Access: 1 December 2018.

Wang, Q., Cao, J., Tao, J., Li, N., Su, X., Chen, L.A., Wang, P., Shen, Z., Liu, S. and Dai, W. (2013). Long-term trends in visibility and at Chengdu, China. *PLoS One* 8: e68894.

WHO (2006). *Who Air Quality Guidelines for Particulate Matter, Ozone, Nitrogen Dioxide and Sulfur Dioxide-Global Update 2005-Summary of Risk Assessment*, 2006. World Health Organization, Geneva, Switzerland.

WMO (2014). *Guide to Meteorological Observing and Information Distribution Systems for Aviation Weather Services*. World Meteorological Organization, Geneva, Switzerland.

WMO (2017). *Manual on Codes: International Codes*, 2011 ed. World Meteorological Organization, Geneva, Switzerland.

Wong, D.K.Y., Pitfield, D.E., Caves, R.E. and Appleyard, A.J. (2006). Quantifying and Characterising aviation accident risk factors. *J. Air Transport Manage.* 12: 352–357.

Xiao, S., Wang, Q.Y., Cao, J.J., Huang, R.J., Chen, W.D., Han, Y.M., Xu, H.M., Liu, S.X., Zhou, Y.Q., Wang, P., Zhang, J.Q. and Zhan, C.L. (2014). Long-Term trends in visibility and impacts of aerosol composition on visibility impairment in Baoji, China. *Atmos. Res.* 149: 88–95.

Yee, T.W. (2018). VGAM: Vector Generalized Linear and Additive Models; 2018. R package version 1.0–6, https://CRAN.R-project.org/package=VGAM

Yu, X., Ma, J., An, J., Yuan, L., Zhu, B., Liu, D., Wang, J., Yang, Y. and Cui, H. (2016). Impacts of meteorological condition and aerosol chemical compositions on visibility impairment in Nanjing, China. *J. Cleaner Prod.* 131: 112–120.

Zhang, S.P., Xie, S.P., Liu, Q.Y., Yang, Y.Q., Wang, X.G. and Ren, Z.P. (2009). Seasonal variations of Yellow Sea fog: Observations and mechanisms. *J. Clim.* 22: 6758–6772.

Zhang, X.Y., Wang, Y.Q., Niu, T., Zhang, X.C., Gong, S.L., Zhang, Y.M. and Sun, J.Y. (2012). Atmospheric aerosol compositions in China: Spatial/temporal variability, chemical signature, regional haze distribution and comparisons with global aerosols. *Atmos. Chem. Phys.* 12: 779–799.

Zhao, H., Che, H., Zhang, X., Ma, Y., Wang, Y., Wang, H. and Wang, Y. (2013). Characteristics of visibility and particulate matter (PM) in an urban area of Northeast China. *Atmos. Pollut. Res.* 4: 427–434.